AIAA Paper 83-1888, July 1983.
[3]Williams, M. H., Bland, S. R., and Edwards, J. W., "Flow Instabilities in Transonic Small-Disturbance Theory," *AIAA Journal*, Vol. 23, No. 10, 1985, pp. 1491–1496.
[4]Fuglsang, D. F., "Nonisentropic Unsteady Transonic Small Disturbance Theory," M.S. Thesis, Purdue Univ., West Lafayette, IN, May 1985.
[5]Whitlow, W., Jr., "XTRAN2L: A Program for Solving the General Frequency Unsteady Transonic Small Disturbance Equation," NASA TM 85723, Nov. 1983.
[6]Dowell, E. H., Bland, S. R., and Williams, M. H., "Linear/Nonlinear Behavior in Unsteady Transonic Aerodynamics," *AIAA Journal*, Vol. 21, 1983, pp. 38–46.
[7]Murty, H. S., "Nonlinear Aspects of Transonic Aeroelasticity," Ph.D. Dissertation, Univ. of Toronto, Ontario, Canada, 1992.
[8]Kerlick, G. D., and Nixon, D., "Mean Values of Unsteady Oscillations in Transonic Flow Calculations," *AIAA Journal*, Vol. 19, No. 11, 1981, pp. 1496–1498.
[9]Dowell, E. H., Ueda, T., and Goorjian, P. M., "Transient Decay Times and Mean Values of Unsteady Oscillations in Transonic Flow," *AIAA Journal*, Vol. 21, No. 12, 1983, pp. 1762–1764.

# Passive Control of Delta Wing Rock

Costas Emmanuel Synolakis,* Brett D. Breuel,†
Murali Tegulapalle,† and Chih-Ming Ho‡
*University of Southern California,*
*Los Angeles, California 90089*

## Introduction

THIS study reports preliminary results on passive control of delta wing rock obtained by adding extended winglets near the leading edge of the wing. The results suggest that the angle of attack at which wing rock occurs can be substantially increased with geometrically simple alternations.

Slender wing rock is a classical problem in aerodynamics; delta wings can provide high-lift forces at relatively large angles of attack. However, their ubiquitous use in high-performance aircraft has been limited by still-existing uncertainties related to their unsteady aerodynamic characteristics,[1] which involve complex, intrinsically three-dimensional separated flows.

One of the first quantitative and analytical studies of the unsteady aerodynamics of delta wing flows at high angles of attacks is that of Ericsson and Reding[2]; using Polhamus[3] leading suction analogy, they concluded that potential-flow theory could be effectively modified to predict adequate results for static loads and that certain unsteady aerodynamics characteristics could be obtained by analyzing the effects of leading-edge vortices. Nguyen et al.[4] focused on the self-induced delta wing rock, a roll oscillation that occurs "naturally" at high angles of attack; with their laboratory results they obtained the now-classic stability boundary relating the limiting angle of attack at which wing rock occurs to the apex angle of the wing. Ericsson[5] confirmed previous observations[4,6] about the two causative separation-induced instabilities; he concluded that large-amplitude delta wing rock is caused by asymmetric leading-edge vortices, while vortex breakdown has a damping effect. He also presented preliminary analytical results for the predictions of wing rock. Recently, Ericsson[7,8] has presented an enhanced comprehensive analytical approach verifying his earlier conclusions.

Received Sept. 30, 1991; revision received Jan. 13, 1992; accepted for publication Jan. 16, 1992. 

*Associate Professor of Aerospace Engineering.
†Laboratory Assistant.
‡Professor of Aerospace Engineering.

Studies of passive control of delta wing rock appear to have been very limited; Katz and Levin[9] showed that a delta wing/canard configuration enhanced the roll oscillation at conditions where the unmodified wing would have been stable. In this study we will report results and describe other modifications, one of which actually enhances the wing-rock stability envelope of certain delta wings.

## Experimental Equipment

The baseline delta wing model we used in this study was a triangular-shaped plane surface with an apex half-angle of 10.1 deg. (This is the quantity usually referred to as $\theta_A$.) The wing thickness was uniform and equal to 0.5 cm; its chord length 23.28 cm and the length of the base of the delta wing was 8.29 cm. The tests were conducted in the USC low-speed wind tunnel with maximum freestream velocities of 23 m/s. Most tests were conducted at a speed of 12 m/s. The test section is 30 × 30 × 90 cm. The wing was mounted on its base through a shaft with an ultralow-friction bearing on a rotary variable differential transformer which measured the amplitude of the oscillation. The geometric arrangement is identical to that used by Levin and Katz,[6] except that the shaft from the RVDT did not extend over any part of the wing surface. Wing rock was diagnosed both from the RVDT output and by visual observations. The baseline wing was used to screen various modifications; the procedure involved increasing the angle of attack until wing rock was initiated. The angle of attack was then further increased to investigate the stability characteristics. After the optimal modification was determined for the baseline wing, wings with different apex angles and identical modifications were tested to determine the stability boundary.

## Laboratory Observations

Several modifications of the baseline delta wing were implemented with the objective to interfere with the vortex formation at the leading edge. The results of these preliminary tests are summarized in Table 1, which compares the critical angle of attack that initiated rock for the different configurations with the critical angle of the baseline wing. The baseline wing is shown in Fig. 1a. In one series of tests (cases 2 and 3), rods of 0.15 cm diam were mounted at the apex at different angles, as shown in Fig. 1b, and then perpendicular to the wing surface at the bottom (case 4), as shown in Fig. 1c. In these tests the motivation was to attempt to produce more symmetric vortex shedding. In another series of tests, a fin was added in the back of the wing as shown in Fig. 1d (cases 5 and 6). Then a series of tests were conducted, where winglets of different sizes and apex-angles were positioned at different distances on either side of the apex of the wing, as shown in Fig. 2 (cases 7–15). These tests indicated that certain sizes of extended winglets resulted in an enhanced envelope of operation. More comprehensive tests were then undertaken to determine the optimal configuration.

Figure 3 shows the stability boundary for the baseline delta wing and the delta wing with extended winglets with a winglet-length to chord-length ratio of 0.43. The ordinate is the angle of attack at which wing rock first appears. The abscissa is the apex half-angle. The figure depicts the curve given in Nguyen et al.[4] (open circles) and the data for the baseline wing obtained in this study (open squares); a comparison of the two curves provides a measure of the errors associated with the laboratory method. The figure also shows the data for the modified wing (solid squares); it is clear that the envelop of operation of the wing is substantially enhanced in the small apex half-angle range. For $\theta_A > 20$ deg the data describes the first occurrence of vortex breakdown. For $\theta_A < 5$ deg, there was no detectable wing rock; the modified wing was unconditionally stable. It is interesting to note that the modified wing curve indicates that similar regimes exist for the modified and unmodified wings.

**Table 1 Summary of the laboratory data; the critical angle of attack which initiates wing rock is tabulated along with the corresponding alteration type**

| Delta wings with apex half-angle; $\lambda$ = 10 deg, chord length = 23.28 cm | | | |
|---|---|---|---|
| Case no. | Figure | Alteration type | Critical angle of attack which initiates wing rock, ±0.2 deg |
| 1 | 1a | Baseline configuration | 31.3 deg |
| | | Rod alterations | |
| 2 | 1b | $\ell$ = 3.8 cm, $\beta$ = 25 deg | 29.4 deg |
| | | Rod alterations | |
| 3 | 1b | $\ell$ = 3.8 cm, $\beta$ = 20 deg | 25.0 deg |
| | | Rod alterations | |
| 4 | 1c | $\ell$ = 1.27 cm, rod perpendicular to the wing plane | 30.9 deg |
| 5 | 1d | Fin on back with $\beta$ = 5 deg | 28.7 deg |
| 6 | 1e | Small fins at the rear with $\beta$ = 20 deg | 30.0 deg |
| | | Winglets at the leading edge | |
| 7 | 2a | $\ell$ = 3.81 cm, $\beta$ = 30 deg | 23.0 deg |
| | | Winglets angle-up | |
| 8 | 2b | $\ell$ = 3.81 cm, $\beta$ = 30 deg, $\theta$ = 13 deg | 24.0 deg |
| | | Winglets angle-down | |
| 9 | 2c | $\ell$ = 3.81 cm, $\beta$ = 30 deg, $\theta$ = 17 deg | 28.0 deg |
| | | Winglets at a distance | |
| | 2d | $a$ = 2.54 cm from the apex | |
| 10 | | $\ell$ = 3.81 cm, $\beta$ = 35 deg | 29.0 deg |
| | | Extended winglets | |
| 11 | 2e | $\ell$ = 23.3 cm, $\beta$ = 10 deg | 43.0 deg |
| | | Extended winglets | |
| 12 | 2e | $\ell$ = 22.4 cm, $\beta$ = 10 deg | 43.0 deg |
| | | Extended winglets | |
| 13 | 2e | $\ell$ = 17.5 cm, $\beta$ = 10 deg | 43.0 deg |
| | | Extended winglets | |
| 14 | 2e | $\ell$ = 14.0 cm, $\beta$ = 10 deg | 43.0 deg |
| | | Extended winglets | |
| 15 | 2e | $\ell$ = 10.0 cm, $\beta$ = 10 deg | 37.0 deg |

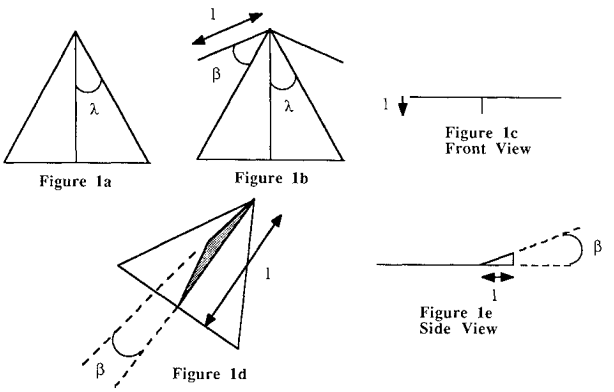


**Fig. 1 Schematic diagrams of delta wings with rod-type alterations.**

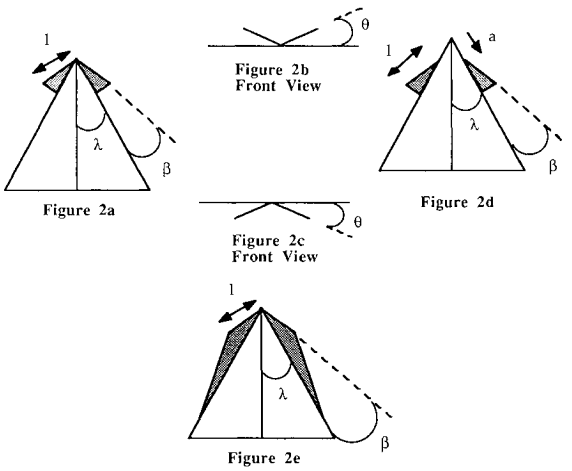


**Fig. 2 Schematic diagrams of delta wings with winglet-type alterations.**

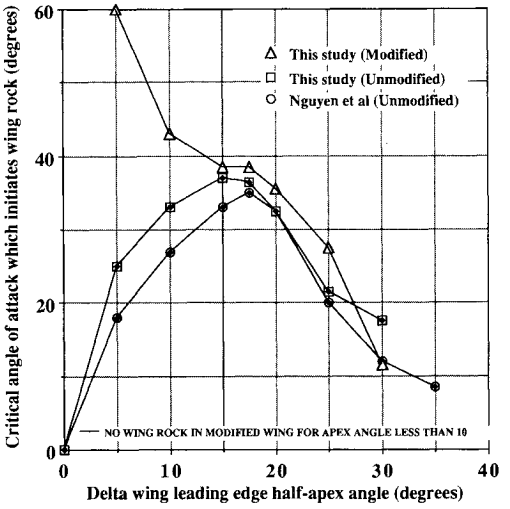


**Fig. 3 Stability diagram for the baseline wing and for the modified wing. The ordinate $\alpha$ is the angle of attack at which rock first appears. The abscissa $\theta_A$ is the apex half-angle of the delta wing. The region of $\theta_A < 20$ deg is the region of asymmetry, while the region of $\theta_A < 20$ deg is the region of vortex burst.**

Without extensive flow visualization data, it is difficult to speculate about the reasons why the extended winglets produce such large differences in the critical angle of attack; however, it is possible that the extended winglets by increasing the effective apex half-angle promote earlier vortex-breakdown, therefore, hindering wing-rock and subsequently increasing the critical angle of attack for incipient wing rock.

## Conclusions

In this note we presented laboratory data that suggest that the critical angle of attack at which wing rock happens is a

phenomenon that is highly dependent on the particular geometric configuration; modified delta wings appear to exhibit similar behavior as unmodified wings and they are dominated by either vortex asymmetry or vortex burst. Extended winglets with a winglet-length to chord-length ratio of 0.43 appear to increase the envelope of operation of the wing substantially in the small apex half-angle region where wing rock occurs. No conclusions can yet be drawn on the relative increase of the drag coefficient over the baseline configuration; however, any adverse effects in the drag coefficient are likely to be outweighed by the benefits of enhanced lift characteristics. These preliminary results indicate that passive control of wing rock may be an effective method for increasing and enhancing the stability of delta wings at high angles of attack.

### Acknowledgments

This research was supported by a Presidential Young Investigator Grant from the National Science Foundation to Costas Synolakis. We are grateful to L. E. Ericsson for many interesting suggestions.

### References

[1]Gad-El-Gak, M., and Ho, C.-M., "The Pitching Delta Wing," *AIAA Journal*, Vol. 23, No. 11, 1985, pp. 1660–1665.

[2]Ericsson, L. E., and Reding, J. P., "Unsteady Aerodynamics of Slender Delta Wings at Large Angles of Attack," *Journal of Aircraft*, Vol. 12, No. 9, 1975, pp. 721–729.

[3]Polhamus, E. C., "Predictions of Vortex Lift Characteristics by a Leading Edge Suction Analogy," *Journal of Aircraft*, Vol. 8, No. 4, 1971, pp. 193–199.

[4]Nguyen, L. T., Ericsson, L. E., Yip, L. P., and Chambers, J. R., "Self-Induced Wing-Rock on Slender Delta Wings," AIAA Paper 81-1883, Aug. 1981.

[5]Ericsson, L. E., "The Fluid Mechanics of Slender Wing Rock," *Journal of Aircraft*, Vol. 21, No. 5, 1984, pp. 323–328.

[6]Levin, D., and Katz, J., "Dynamic Load Measurements of Delta Wings Undergoing Self-Induced Roll Oscillations," *Journal of Aircraft*, Vol. 21, No. 9, 1984, pp. 30–36.

[7]Ericsson, L. E., "Analytic Predictions of the Maximum Amplitude of Slender Wing Rock," *Journal of Aircraft*, Vol. 26, No. 1, 1989, pp. 35–39.

[8]Ericsson, L. E., "Slender Wing-Rock Revisited," AIAA Paper 91-0417, Jan. 1991.

[9]Katz, J., and Levin, D., "Self-Induced Roll Oscillations Measured on a Delta Wing/Canard Configuration," *Journal of Aircraft*, Vol. 23, No. 11, 1989, pp. 815–819.

# Computational Method for Matching Aerodynamic Experimental Data with Theoretical Influence Matrices

Claudio Ponzi*
*Alenia, Rome, Italy*

### Nomenclature

$[A]$ = aerodynamic influence matrix
$AR$ = wing aspect ratio
$a_{ij}$ = generic element of $[A]$
$I_i$ = performance index, defined for each aerodynamic center point
$L$ = number of matched coefficients per aerodynamic center point
$N$ = order of $[A]$
$S_1$ = set of aerodynamic coefficients which must fit experimental results
$S_2$ = set of aerodynamic coefficients assumed not to need any correction
$s$ = wing semispan
$t$ = wing aspect ratio
$(\boldsymbol{\alpha})$ = vector of panel angles of attack on control points
$(\Delta \boldsymbol{c}_p)$ = differential pressure coefficient vector across the aerodynamic panel
$\Lambda$ = wing sweep
$\tau$ = theoretical grid point location on the wing semispan axis

Received Aug. 31, 1991; revision received Dec. 30, 1991; accepted for publication Jan. 2, 1992. 

*Aerospace Engineer, Corporate Research and Development Department.

### Introduction

AERODYNAMIC influence matrices relate local aerodynamic pressure coefficients at collocated grid points and local angles of attack at some other (different) grid points. They are obtained, e.g., through the so-called panel methods. Some examples are the HISSS[1] Code and the "vortex lattice method."[2,3] Panel methods are suitable for studying both subsonic and supersonic flows in steady and unsteady conditions. The latter case leads to frequency-domain airloads, i.e., angles of attack and aerodynamic matrices that are frequency-dependent quantities. All of the following developments are valid within this unsteady flow frame as well.

Panel methods compare well with experimental data provided that the flow conditions are in good agreement with the implicit assumptions of the linearized potential flow model. The purpose of this work is to analyze how experimental pressure data can be used to improve the agreement between theory and experiment, thereby enhancing the use of numerical results.

### Solution Procedure

In this article, the term "similar aerodynamic grid" means 1) similar wing planform (same aspect ratio, same sweep angle, same thickness percentage together with equal Mach number); and 2) equal distribution of aerodynamic center points and control points at defined chordwise and spanwise percentage locations. The case in which the theoretical and experimental aerodynamic grids are similar is examined first.

In a linear aerodynamic theory, the aerodynamic influence matrix relates the differential pressure coefficient vector $(\Delta \boldsymbol{c}_p)$ and the vector of panel angles of attack $(\boldsymbol{\alpha})$ in the following form:

$$(\Delta \boldsymbol{c}_p) = [A](\boldsymbol{\alpha}) \tag{1}$$

Expanding Eq. (1) one obtains

$$\Delta \boldsymbol{c}_{pi} = \sum_{j=1}^{N} a_{ij} \boldsymbol{\alpha}_j \tag{2}$$

One can split Eq. (2) into two contributions, according to the fact the theoretical matrix $[A]$ is supposed to fit a set of experimental results

$$\Delta \boldsymbol{c}_{pi} = \sum_{n \in S_1} a_{in} \boldsymbol{\alpha}_n + \sum_{m \in S_2} a_{im} \boldsymbol{\alpha}_m \tag{3}$$

where $S_1$ has to be interpreted as the set of coefficients which must fit experimental results, while $S_2$ represents the set of the remaining theoretical coefficients. Assuming the $S_2$ coefficients to be known, they can be put on the right side of Eq. (3) together with $\Delta \boldsymbol{c}_{pi}$. The number of elements of $S_1$ (respectively $S_2$) is $L$ (respectively $N - L$) and the upper bound for $L$ is the number of linearly independent aerodynamic settings of the aircraft (equal to the single movable surface unit deflections and the global unit angle of attack). When solving Eq. (3), a maximum of $L$ unknown influence coefficients can be taken into account for each row $i$ of the system: